iScience

Article

Alpha power indexes working memory load for durations

Graphical abstract

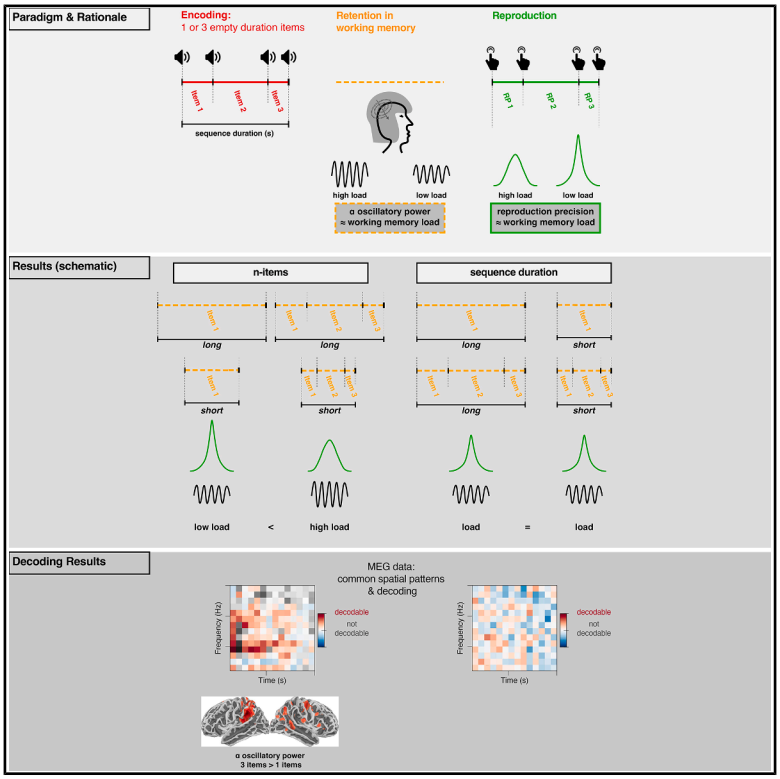

Highlights

- Higher working memory load, induced by more duration items, reduced recall precision
- Alpha power, a known signature of working memory load, indexed load caused by durations
- Alpha power over parietal regions during retention mediated behavioral recall precision
- The results suggest that durations are stored in working memory in the form of abstract items

Authors

Sophie K. Herbst, Izem Mangione, Charbel-Raphaël Segerie, Richard Höchenberger, Tadeusz Kononowicz, Alexandre Gramfort, Virginie van Wassenhove

Correspondence

ksherbst@gmail.com (S.K.H.), virginie.van.wassenhove@gmail.com (V.v.W.)

In brief

Biological sciences; Neuroscience; Cognitive neuroscience

Herbst et al., 2026, iScience *29*, 114212
January 16, 2026
https://doi.org/10.1016/j.isci.2025.114212

CellPress

iScience

CellPress
OPEN ACCESS

Article

Alpha power indexes working memory load for durations

Sophie K. Herbst,[1,5,*] Izem Mangione,[1] Charbel-Raphaël Segerie,[2] Richard Höchenberger,[2] Tadeusz Kononowicz,[1,3,4] Alexandre Gramfort,[2] and Virginie van Wassenhove[1,*]

[1]Cognitive Neuroimaging Unit, INSERM, CEA, Université Paris-Saclay, NeuroSpin, 91191 Gif-sur-Yvette, France
[2]Inria, CEA, Université Paris-Saclay, Palaiseau, France
[3]Institute of Psychology, The Polish Academy of Sciences, ul. Jaracza 1, 00-378 Warsaw, Poland
[4]Institut NeuroPSI - UMR9197, CNRS, Université Paris-Saclay, Gif-sur-Yvette, France
[5]Lead contact
*Correspondence: ksherbst@gmail.com (S.K.H.), virginie.van.wassenhove@gmail.com (V.v.W.)
https://doi.org/10.1016/j.isci.2025.114212

SUMMARY

Estimating and comparing how long events last requires the temporary storage of durations. How durations are stored in working memory is unknown, despite the central role of memory systems in timing. We investigated the neural signatures of working memory for sequences of durations with magnetoencephalography (MEG) while human participants performed an n-item delayed reproduction task. Sequences orthogonally varied in the number of items (one or three) and their durations. The number of durations in the sequence, but not the duration of the sequence, affected recall precision and could be decoded from alpha and beta oscillatory activity during retention. Our results extend earlier behavioral findings, suggesting that durations are itemized in working memory and that their number, not their duration, modulates recall precision. Crucially, we establish that alpha power reflects a universal signature of working memory load and mediates recall precision, even for abstract information such as duration.

INTRODUCTION

Humans and animals can readily discriminate the durations of sensory events as well as the silent intervals that may separate them. Sensory timing tasks typically quantify this ability by asking individuals to compare or (re)produce time intervals.[1] In most sensory timing tasks, the encoded temporal information is stored until a decision is made: for instance, in the simplest two-alternative forced-choice design, two time intervals are presented in succession, and the first of the two is held in working memory until the second is presented and a comparison can be made.[2–4] The encoding of duration in such tasks and the decision stages have been well explored.[5–7] To the contrary, how durations are maintained in working memory is unknown. Classical information-theoretic timing models postulated a working memory component,[8–11] but its mechanisms and neural dynamics remain largely speculative.[12–14]

Recent behavioral work suggests that the storage of durations in working memory is comparable to that of any items,[15–17] in that recall precision is indicative of working memory load.[18–20] At the cortical level, the maintenance of encoded events in working memory has been linked to oscillatory dynamics,[21] which provide a self-sustained neural code in the absence of sensory stimulation. Working memory function likely relies on different oscillatory regimes, ranging from theta to alpha, beta, and gamma.[22–27] A consistent finding is that alpha power (8–12 Hz) increases with working memory load,[28] but studies assessing working memory for duration do not clearly align with this seminal observation as discussed below.[29,30]

Herein, we thus investigated whether duration storage follows the known principles of working memory. We focused on recall precision as a measure of working memory load and neural oscillations as its neural signature. We recorded participants' brain activity with magnetoencephalography (MEG) while they performed an n-items delayed reproduction task, in which they were asked to encode, maintain, and reproduce temporal sequences of varying length. Critically, we orthogonalized the number of items (one or three) in a sequence and the duration of the sequence. Using this task, we previously showed that the number of items, but not the duration of the sequence, affected recall precision.[15] These results provided evidence that durations can be itemized and stored in working memory as mental abstract magnitudes.[31–34] Accordingly, in the present study, we expected an increase in alpha power, with working memory load depending on the number of durations in a sequence but not on the duration of the sequences itself.

The modulation of alpha power is a well-established marker of working memory load, resulting from the number of items.[28,35,36] Jensen et al. (2002) demonstrated a parametric alpha increase over posterior and parietal regions during a visual Sternberg task (2, 4, and 6 items, electroencephalography [EEG]), a finding that has since been replicated in visual[37–39] and auditory contexts[40–43] (see also the review by Wilsch et al.).[44] Working memory load is classically operationalized through the number of

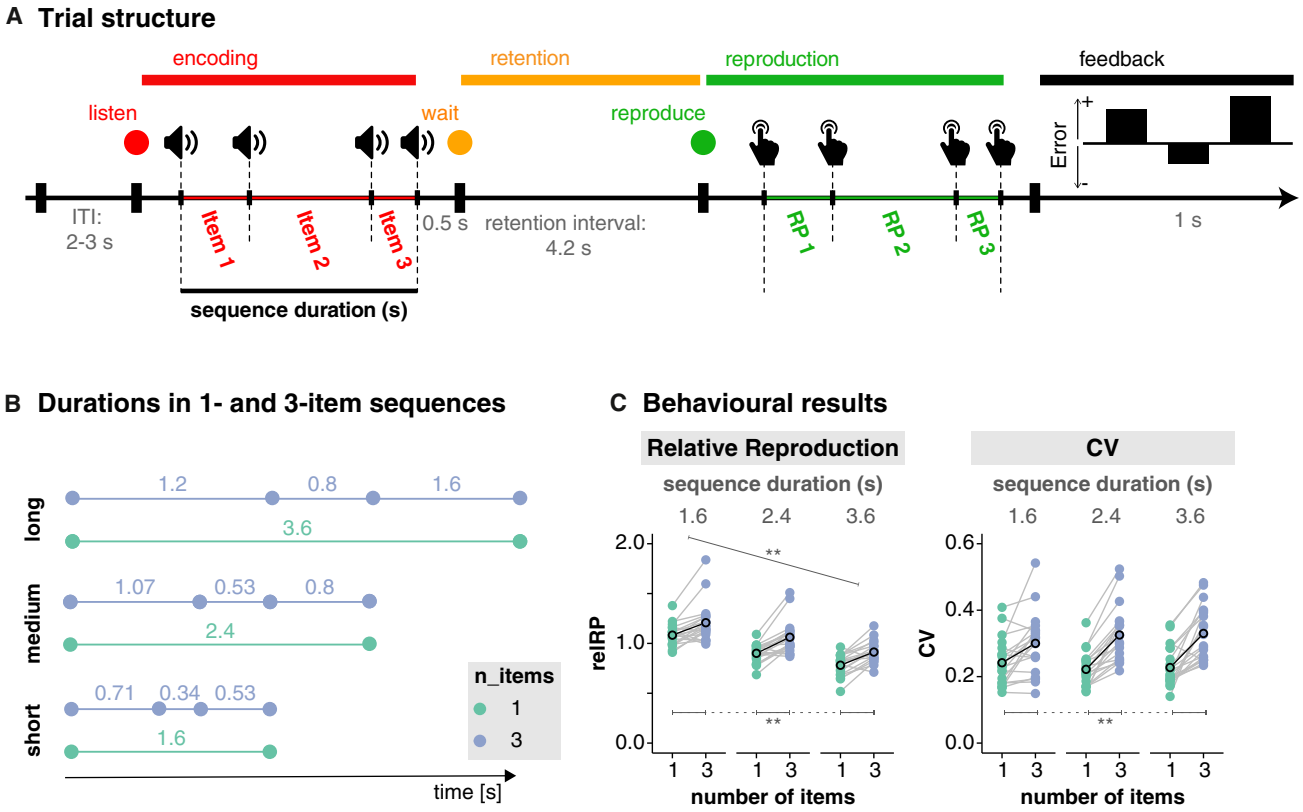

Figure 1. N-item delayed reproduction task and behavioral results

(A) Trial structure. Each trial consisted of four phases. First, participants listened to a sequence of pure tones (1 kHz, 50 ms) demarcating empty time intervals of varying duration (encoding phase, red fixation dot). Following a retention interval (orange fixation dot), participants were asked to reproduce the full temporal sequence as precisely as possible (green fixation dot). In the example depicted here, the sequence was composed of three durations. Following their reproduction, participants received feedback about the relative temporal reproduction error for each duration in the sequence. ITI, inter-trial-interval; RP, reproduction.

(B) Items and sequences. Dots represent tones. Horizontal lines and the numbers above indicate the duration of the empty intervals in seconds. A sequence was composed of one or three items (blue and green, respectively). The durations of sequences were fixed to 1.6 s (short), 2.4 s (medium), or 3.6 s (long), irrespective of the number of items that composed them, such that the number of items and the duration of the full sequence were orthogonalized.

(C) Effects of the number of items and the duration of sequences on relative reproduction (relRP) and inverse precision (coefficient of variation, CV). Left: relRP significantly increased with the number of items and decreased with the duration of the sequence (** = $p < 0.01$, fixed effect in linear mixed effect model). Right: CVs were not affected by the duration of the sequence but significantly increased with the number of items, indicating a decrease in reproduction precision with higher working memory load.

items that have to be maintained, but similar results have been obtained when modulating the complexity of the stimuli.[43,45,46]

The increase in alpha power is thought to reflect inhibition of task-irrelevant information during retention[47] (see also[48,49]) and can be modulated by temporal expectations about the retention interval.[50,51] Two studies have directly targeted the neural dynamics of working memory maintenance for duration: one study showed that alpha power decreased with longer visual item durations,[29] whereas the second study, using a visual n-back task, reported a decrease in posterior alpha power with increasing working memory load—together with beta power increase over temporal areas.[30] The divergent alpha power trends in timing studies suggest the possibility of distinct mechanisms for durations held in working memory. To investigate this further, we employed alpha power as an index of working memory load, aiming to determine which factor, the number of items (n-items), or the duration of the sequence contributes most to working memory load.

We show that the number of items, but not the duration of the sequence, can be decoded from both alpha and beta (15–25 Hz) band activities, with distinct cortical sources. Interestingly, the alpha-band power showed a direct link to the precision of temporal reproduction. Thus, our results suggest that durations are itemized in working memory like any other mental events.

RESULTS

Behavioral results

In an n-item-delayed-reproduction task, participants reproduced sequences of either one or three duration items following a retention interval (see Figure 1A). The sequences varied orthogonally in the number of items (one or three) and the duration of the sequence (1.6 s/short, 2.4 s/medium, and 3.6 s/long; Figure 1B). The behavioral results replicate our previous findings.[15] Specifically, the relative reproduction (relRP, defined as

Table 1. Effects of the number of items (n-item) and sequence duration on the relative reproduction (relRP) and precision (CV) of temporal reproductions

DV	IV	STAT	*p*	BF
relRP	**n-item**	**F(1, 19) = 27.58**	**<0.001**	**>1000**
	sequence duration	**F(1, 19) = 173.02**	**<0.001**	**>1000**
	IA	F(1, 25) = 0.01	0.95	<0.001
CV	**n-item**	**F(1, 19) = 45.94**	**< 0.001**	**> 1000**
	sequence duration	F(1, 19) = 0.51	0.49	0.013
	IA	F(1, 19) = 6.41	0.02	0.018

Bayes factors (BF) reflect the Bayesian evidence for the significance of the respective predictor. Bold values indicate a significant effect. DV, dependent variable; IV, independent variable; STAT, statistical parameters; P, *p*-value; IA, interaction.

the ratio between each item's reproduction and duration) was modulated by the number of items and the sequence duration (Table 1; Figures 1C and S1). Consistent with context effects in magnitude estimation,[52] durations in sequences containing more items were reproduced as longer compared to durations that occurred alone. Furthermore, short sequences were overproduced and long sequences underproduced, an effect typically interpreted as a regression to the mean.[52–54]

More importantly, the results confirm that the number of items significantly decrease the precision of temporal reproduction [quantified as the coefficient of variation, CV: mean (item reproduction) divided by standard deviation (item reproduction); $F(1, 19) = 45.94$, $p < 0.001$, BF10 > 1,000]. Conversely, the duration of the sequence did not significantly affect the precision of temporal reproduction [$F(1, 19) = 0.51$, $p = 0.49$, BF10 = 0.13]. Thus, the number of durations, but not the duration of the sequence itself, constitutes the load when it comes to storing multiple durations in working memory.

Decoding results

Next, we applied common spatial pattern decoding (CSP)[55,56] on the MEG data to test whether oscillatory dynamics during the stimulus-free retention interval contained information about the number of items and/or the duration of the sequence. Decoding was applied to induced oscillatory power (after subtraction of the evoked response), and in time-frequency bins (2–25 Hz, 0.5–4 s). Significant decoding performance at the group level was observed only for the number of items (Figure 2A, left) but not for the duration of the sequence (Figure 2B; Standard error of the mean for the time-frequency matrices is displayed in Figure S2.) A cluster permutation test revealed a statistically significant cluster spanning all time-frequency bins (Figure 2A, left). The peak frequency distributions (histograms in Figure 2A, middle) were of bimodal shape, with one peak in the alpha and one in the beta band. The source projection of the decoding patterns for the whole frequency and time ranges showed sources in occipital, parietal, and motor areas (Figure 2C). To investigate the cortical dynamics underlying the significant decoding performance, we separated the decoding patterns in the alpha and beta bands before projecting the weights in source space (Figure 2E). This revealed parieto-occipital sources in the alpha band versus a more pronounced spread into sensorimotor areas for the beta band. Both were relatively lateralized to the left hemisphere. Lastly, we reconstructed the sources directly from the oscillatory power, rather than from the decoding patterns, which allowed assessing the directionality of the effect: for the alpha band, we observed higher power for three-item versus one-item sequences, with a bilateral occipital distribution. In the beta band, power was higher for one-item compared to three-item sequences in the motor regions and higher for three-item sequences in occipital regions (Figure 2F), both bilateral. While the effect of beta power in the occipital regions likely reflects harmonics of alpha, the opposite directionality and the different topographical distributions of the modulation of beta power in the sensorimotor areas suggests that it reflects an independent effect. These findings thus argue for the separability of alpha and beta dynamics during working memory maintenance.

Alpha power mediates the effect of n-items on precision

We addressed the relationship between the precision of reproduction (quantified by the CV, computed for single trials through a resampling and bootstrapping approach; see STAR Methods) and oscillatory power in the alpha and beta bands, obtained from six source labels covering the significant decoding patterns: lateral occipital cortex, inferior parietal cortex, superior parietal cortex, supramarginal gyrus, precentral gyri, and postcentral gyri (all bilateral). Alpha power in the bilateral superior parietal cortices, supramarginal gyri, and postcentral cortex showed a significant relationship with CV in the one-item trials (correlations ranging from −0.057 to −0.068, all $p < 0.003$; Figure 2D; see also Table S1 and Figure S3): CV decreased with higher alpha power, meaning precision increased. A marginally significant correlation was observed in the inferior parietal areas ($r = -0.053$, $p = 0.006$). No significant effects were found in the three-item trials, nor for the beta band (all $p > 0.02$). We then tested for a direct relationship between the behavioral precision effects and the differences in oscillatory dynamics for 3- vs. 1-item through mediation.[57] Alpha power in bilateral supramarginal gyrus mediated the effect of n-items on precision: (1) the independent variable n-items had a significant effect on the mediator, power (*a* effect; −0.06 [−0.07 to −0.06], bootstrapped 95% confidence interval); (2) n-items significantly affected the CV (*b* effect, −0.1 [−0.17 to −0.04]); and (3) the indirect path of n-items on CV via power was significant ($a \times b$ effect, 0.01 [0.0–0.01]).

In sum, alpha power in the supramarginal gyrus mediated the effect of the number of items on the precision of temporal reproduction, suggesting that working memory load increases with the number of durations, not with the duration of the sequence.

DISCUSSION

Sustained representations of durations are required for tasks like duration comparison or reproduction,[58] but little is known about duration storage in memory. Here, we investigated whether working memory for duration follows similar principles as working memory for sensory items.[15,16,19,20,59,60] Specifically, we assessed established behavioral and neural markers of working memory maintenance from the sensory domain, namely recall

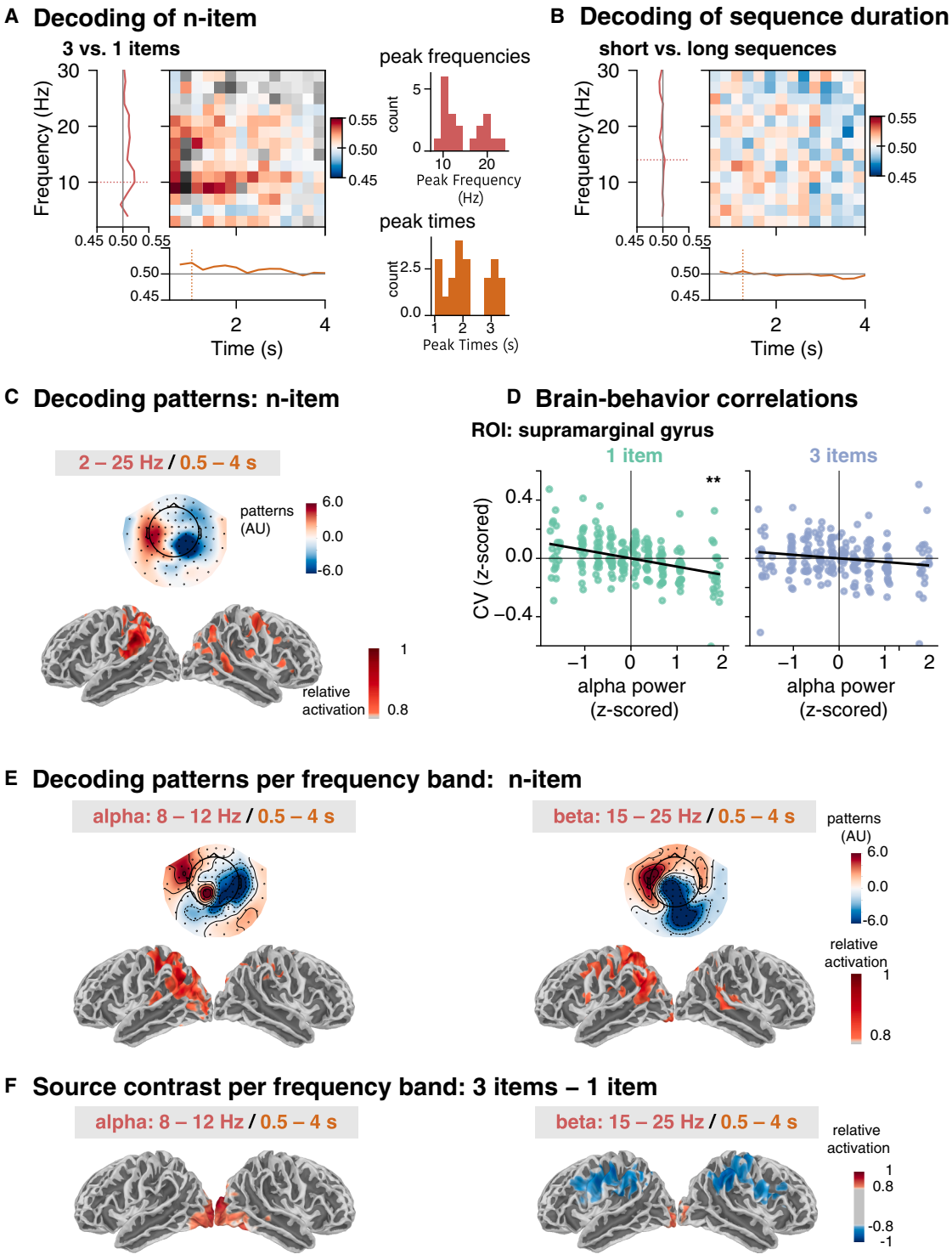

Figure 2. MEG decoding

(A) N-item decoding in sensor space. The number of items was significantly decoded from induced power in the alpha and beta bands during the retention interval using common spatial patterns (CSP). Left: decoding performance during the retention interval, computed in time-frequency bins. The colored pixels reflect significant decoding performance (decoding accuracy > 0.5; cluster permutation test) and the gray ones non-significant decoding performance. The marginal means reflect average decoding performance across frequency (left, red) and time points (below, orange). Middle: the red and orange histograms show the frequencies and latencies with the highest decoding performance for each participant.

(legend continued on next page)

precision and neural oscillatory power during retention, to test whether working memory load for durations is driven by the number of durations (n-items) or their total duration (i.e., temporal extent) itself. Manipulating n-items and sequence duration orthogonally in a previously published n-item delayed reproduction task,[15] we replicated our previous behavioral findings that recall precision decreased with the number of items but not with sequence duration (Figure 1).

During working memory maintenance, a decoding approach applied to MEG data revealed that induced oscillatory dynamics (parieto-occipital alpha and sensorimotor beta) reflected the number of durations (3- vs. 1-item), but not the duration of the sequence (Figure 2). Furthermore, alpha power statistically mediated the effect of n-items on behavioral precision. A key contribution of this work is the demonstration that time intervals are represented as discrete items in working memory, which extends the principles of sensory working memory to abstract temporal information.[15,31,33,34]

Alpha power indexes working memory load

Maintaining three versus one duration in working memory increased alpha power over parieto-occipital areas. Previous studies have established that maintaining multiple distinct visual or auditory items (e.g., letters, faces, or spoken syllables) in working memory is associated with an increase in alpha power measured over parieto-occipital regions, proportional to working memory load.[28,35,36,39,40,43] Some studies also reported the opposite direction but specifically as a relatively short-lived response to visuo-spatial displays.[61–63] The increase of alpha activity is typically interpreted as the disengagement of the dorsal visual stream, to shield the currently retained information from interference by distracting inputs.[45,47,48,64–66] Our observation extends the signature of alpha power to the maintenance of duration information in working memory. The parietal sources are in line with a previous study reporting load-depended activity modulations in inferior parietal cortex[67] and, more generally, the representation of mental magnitudes in parietal cortices[31] and of durations in chronotopic maps in parietal and motor areas.[68,69]

It has previously been suggested that alpha power could be a signature of spatial attention allocated to more locations with a larger number of items.[70,71] Participants did not mention spatialization as a particular strategy during debriefing, and the most common strategy in timing tasks is counting.[72] Had participants spatialized individual items during retention, subjective distances should increase with item duration according to the classical tau effect,[73] which in turn should have surfaced as an effect of sequence duration (similarly for counting), which was not observed.

Critically, alpha power in the supramarginal gyrus statistically mediated the effect of the number of items on recall precision, providing a direct link between the behavioral precision effect and alpha power as an index for working memory load. Furthermore, the absence of a similar effect on alpha power with longer sequence duration, and the inability to decode sequence duration during retention, corroborate the behavioral result that working memory precision depends solely on the number of duration items.

The role of beta power during working memory retention

Beta power in sensorimotor cortices during retention *decreased* with the number of durations maintained in working memory, which suggests a clear functional distinction from the neural dynamics observed in alpha power over parieto-occipital areas. Beta oscillations are a known neural correlate of working memory,[21,74–76] with several putative functional roles: top-down inhibition,[74,77] with commonalities and overlaps to alpha dynamics, but also more specifically the maintenance of sequence order.[21,77,78] Furthermore, beta power modulations have been reported as neural signatures of interval timing[79–81] and timing precision (modulated by alpha phase[82]), as well as working memory for duration of a single tactile stimulus.[83]

In line with the inhibitory role of beta, our observation of higher beta power for 1-item here might indicate stronger movement inhibition[84–87] or enhanced preparation for target encoding,[77] as the maintenance of single items binds less resources than for multi-item sequences. Furthermore, increased complexity in the motor demands (as in the reproduction of several items) could decrease beta power contralateral to the effector side in a motor imagery task,[88] in line with the left lateralization observed in the source-reconstructed decoding patterns (Figure 2B).

With respect to the specific relevance of beta dynamics to timing, our findings point toward a sustained representation of duration in sensorimotor areas used for working memory maintenance. Seminal investigations revealed that working memory maintenance relies on persistent firing of distributed neural populations, both in areas that encode the respective stimuli (i.e., visual or motor cortices) and in parietal and frontal areas.[18,89] Critically, the amplitude of the activity specifically related to the memorized items decreases with load,[90] as does recall precision. This decrease can be linked to a more distributed representation of multiple items, suggested to be mediated by beta

(B) Decoding of sequence duration (short vs. long). Time-frequency matrix of decoding performance, with marginal means reflecting average decoding performance across frequency (left, red), and time points (below, orange). No significant decoding performance was observed for sequence duration.
(C) Sensor topographies and source projections of decoding patterns, averaged across participants. AU, absolute units.
(D) Brain-behavior correlations. We tested whether the power modulations were directly related to the precision of temporal reproductions per trial. A significant relationship between precision (CV, computed through resampling) and alpha power was found, here depicted for the supramarginal gyrus (sig. only for 1-item; measures were binned only for visualization; $^{**}p < 0.01$, non-parametric resampling).
(E) Sensor topographies and source projections of decoding patterns, separately for the alpha (8–12 Hz) and beta (15–25 Hz) bands. Decoding patterns in the alpha and beta band overlapped but were relatively more shifted to occipital/parietal areas for alpha and central areas for beta and left-lateralized.
(F) Source contrasts for 3- versus 1-item sequences: power differences projected in source space and thresholded at 80%. While panels A and B show the decoding patterns (red = decoding better than chance), which do not allow to infer the directionality of the effect, the contrast of relative power between 3- and 1-item sequences allows to appreciate the different directions of the effects in the alpha (red = more power for three items) and beta bands (blue = more power for one item).

power.[75,91] Here, the successful decoding of the number of durations in working memory from beta band activity points toward a distributed representation of item durations mediated by beta dynamics.

In conclusion, we addressed how sequences of durations are stored in working memory, through behavioral and neural indices of working memory load: recall precision and neural oscillatory dynamics. The number of duration items but not the duration of the sequence had an effect on recall precision and was decodable from oscillatory power in the alpha and beta bands, pointing toward an abstract representation of *duration items* in working memory. Alpha power increased with load, bridging between durations and other kinds of items. Beta power dynamics differed from alpha, suggesting a specialized neural code for duration.

Limitations of the study

Here, we tested only a single type of empty duration items. Future studies should address the generalizability of the findings by using filled durations with delimiters from different modalities and with varying content. Furthermore, the results are mainly of correlational nature, despite the statistical assessment of a mediation effect of the number of items on recall precision by alpha power. Future studies could use perturbational methods such as frequency-specific transcranial alternating current stimulation (tACS) to perturb working memory storage and confirm the causal implication of alpha oscillations in retention. Finally, we did not assess other known signatures of working memory, such as theta, beta, or gamma oscillations,[22,27] which could provide additional insights.

RESOURCE AVAILABILITY

Lead contact

Further information and requests for resources and information should be directed to and will be fulfilled by the lead contact, Sophie Herbst (ksherbst@gmail.com).

Materials availability

This study did not generate new unique reagents.

Data and code availability

- Behavioral data are available on the Open Science Framework, identifier: https://doi.org/10.17605/OSF.IO/P6M7S. The anonymized MEG data including behavioral markers (BIDS format) are available on OpenNeuro, identifier: https://doi.org/10.18112/openneuro.ds006720.v1.0.0.
- Custom code written in python is available on the Open Science Framework, identifier: https://doi.org/10.17605/OSF.IO/P6M7S.
- Any additional information required to reanalyze the data reported in this paper is available from the lead contact upon request.

ACKNOWLEDGMENTS

This project has received funding from Agence Nationale de la Recherche AutoTime (ANR-16-CE37-0004-04) (to V.v.W.), Agence Nationale de la Recherche meegBIDS.fr (ANR-19-DATA-0023) (to A.G. [Coordinator], S.H., Maximilien Chaumon, and V.v.W. (collaborators)], and the European Union's Horizon 2020 research and innovation program under grant agreement no. 101017727 and FET Experience (to V.v.W.).

NeuroSpin, NeuroPSI, UNICOG, Cognition & Brain Dynamics, and the Mind Lab are part of the DIM C-BRAINS, funded by the Conseil Régional d'Ile-de-France. We would also like to thank the NeuroSpin MEG platform staff, and in particular Leila Azizi, for their support during data acquisition. We thank Yunyun Shen for enriching discussions about the study, both theoretically and empirically.

AUTHOR CONTRIBUTIONS

V.v.W., S.K.H., and T.W.K. developed the research concept and study design, to which I.M. also contributed. Coding was performed by S.K.H., I.M., and T.W.K. Testing and data acquisition was performed by I.M. The analyses were performed by I.M., T.W.K., and S.K.H. (behavior, MEG preprocessing); finalized by C.-R.S. and R.H.; and supervised by A.G. and S.K.H. (decoding, source reconstruction), with regular inputs and guidance from V.v.W. S.K.H. wrote the first draft, and S.K.H. and V.v.W. revised the manuscript. All authors reviewed and approved the final version of the manuscript.

DECLARATION OF INTERESTS

The authors declare no competing interests.

DECLARATION OF GENERATIVE AI AND AI-ASSISTED TECHNOLOGIES IN THE WRITING PROCESS

Claude Sonnet 4 was used to optimize Python code. Google Gemini (2.5 Flash) was used to refine English writing. The authors reviewed and edited the content as needed and take full responsibility for the content of the publication.

STAR★METHODS

Detailed methods are provided in the online version of this paper and include the following:

- KEY RESOURCES TABLE
- EXPERIMENTAL MODEL AND STUDY PARTICIPANT DETAILS
- METHOD DETAILS
  - General procedure and task
  - Stimuli
  - MEG recording
  - Anatomical MRI recordings
- QUANTIFICATION AND STATISTICAL ANALYSIS
  - Software
  - Behavioral data
  - MEG preprocessing
  - Anatomical MRI preprocessing and forward model computation
  - Common spatial pattern decoding
  - Source reconstruction
  - Brain-behavior relationships
  - Mediation analyses

SUPPLEMENTAL INFORMATION

Supplemental information can be found online at https://doi.org/10.1016/j.isci.2025.114212.

Received: June 2, 2025
Revised: September 26, 2025
Accepted: November 20, 2025
Published: November 25, 2025

REFERENCES

1. Grondin, S. (2010). Timing and time perception: A review of recent behavioral and neuroscience findings and theoretical directions. Atten. Percept. Psychophys. *72*, 561–582.

2. Coull, J.T., Nazarian, B., and Vidal, F. (2008). Timing, Storage, and Comparison of Stimulus Duration Engage Discrete Anatomical Components of a Perceptual Timing Network. J. Cogn. Neurosci. *20*, 2185–2197.
3. Harrington, D.L., Zimbelman, J.L., Hinton, S.C., and Rao, S.M. (2010). Neural modulation of temporal encoding, maintenance, and decision processes. Cereb. Cortex *20*, 1274–1285.
4. Rao, S.M., Mayer, A.R., and Harrington, D.L. (2001). The evolution of brain activation during temporal processing. Nat. Neurosci. *4*, 317–323.
5. Díaz, H., Bayones, L., Alvarez, M., Andrade-Ortega, B., Valero, S., Zainos, A., Romo, R., and Rossi-Pool, R. (2025). Contextual neural dynamics during time perception in the primate ventral premotor cortex. Proc. Natl. Acad. Sci. USA *122*, e2420356122.
6. Ofir, N., and Landau, A.N. (2022). Neural signatures of evidence accumulation in temporal decisions. Curr. Biol. *32*, 4093–4100.e6.
7. Paton, J.J., and Buonomano, D.V. (2018). The Neural Basis of Timing: Distributed Mechanisms for Diverse Functions. Neuron *98*, 687–705.
8. Buhusi, C.V., and Meck, W.H. (2005). What makes us tick? Functional and neural mechanisms of interval timing. Nat. Rev. Neurosci. *6*, 755–765.
9. Treisman, M. (1963). Temporal discrimination and the indifference interval: Implications for a model of the 'internal clock'. Psychol. Monogr. *77*, 1–31.
10. Gibbon, J. (1977). Scalar expectancy theory and Weber's law in animal timing. Psychol. Rev. *84*, 279–325.
11. Gibbon, J., Church, R.M., and Meck, W.H. (1984). Scalar timing in memory. Ann. N. Y. Acad. Sci. *423*, 52–77.
12. Gu, B.-M., van Rijn, H., and Meck, W.H. (2015). Oscillatory multiplexing of neural population codes for interval timing and working memory. Neurosci. Biobehav. Rev. *48*, 160–185.
13. Teki, S., Gu, B.-M., and Meck, W.H. (2017). The Persistence of Memory: How the Brain Encodes Time in Memory. Curr. Opin. Behav. Sci. *17*, 178–185.
14. van Wassenhove, V. (2016). Temporal cognition and neural oscillations. Curr. Opin. Behav. Sci. *8*, 124–130.
15. Herbst, S.K., Mangione, I., Kononowicz, T., Shen, Y., and van Wassenhove, V. (2025). Abstracting time in memory. J. Exp. Psychol. Learn. Mem. Cogn. *51*, 1576–1593.
16. Manohar, S.G., and Husain, M. (2016). Working Memory for Sequences of Temporal Durations Reveals a Volatile Single-Item Store. Front. Psychol. *7*, 1655.
17. Teki, S., and Griffiths, T.D. (2014). Working memory for time intervals in auditory rhythmic sequences. Front. Psychol. *5*, 1329.
18. Bays, P.M. (2015). Spikes not slots: noise in neural populations limits working memory. Trends Cogn. Sci. *19*, 431–438.
19. Bays, P.M., Schneegans, S., Ma, W.J., and Brady, T.F. (2024). Representation and computation in visual working memory. Nat. Hum. Behav. *8*, 1016–1034.
20. Ma, W.J., Husain, M., and Bays, P.M. (2014). Changing concepts of working memory. Nat. Neurosci. *17*, 347–356.
21. Miller, E.K., Lundqvist, M., and Bastos, A.M. (2018). Working Memory 2.0. Neuron *100*, 463–475.
22. Axmacher, N., Henseler, M.M., Jensen, O., Weinreich, I., Elger, C.E., and Fell, J. (2010). Cross-frequency coupling supports multi-item working memory in the human hippocampus. Proc. Natl. Acad. Sci. USA *107*, 3228–3233.
23. Jensen, O., and Lisman, J.E. (2005). Hippocampal sequence-encoding driven by a cortical multi-item working memory buffer. Trends Neurosci. *28*, 67–72.
24. Kopell, N., Whittington, M.A., and Kramer, M.A. (2011). Neuronal assembly dynamics in the beta1 frequency range permits short-term memory. Proc. Natl. Acad. Sci. USA *108*, 3779–3784.
25. Lisman, J.E., and Idiart, M.A. (1995). Storage of 7 ± 2 Short-Term Memories in Oscillatory Subcycles. Science *267*, 1512–1515.
26. Palva, S., and Palva, J.M. (2011). Functional roles of alpha-band phase synchronization in local and large-scale cortical networks. Front. Psychol. *2*, 204.
27. Roux, F., and Uhlhaas, P.J. (2014). Working memory and neural oscillations: alpha–gamma versus theta–gamma codes for distinct WM information? Trends Cogn. Sci. *18*, 16–25.
28. Jensen, O., Gelfand, J., Kounios, J., and Lisman, J.E. (2002). Oscillations in the Alpha Band (9–12 Hz) Increase with Memory Load during Retention in a Short-term Memory Task. Cereb. Cortex *12*, 877–882.
29. Chen, Y.G., Chen, X., Kuang, C.W., and Huang, X.T. (2015). Neural oscillatory correlates of duration maintenance in working memory. Neuroscience *290*, 389–397.
30. Chen, Y., and Huang, X. (2016). Modulation of Alpha and Beta Oscillations during an n-back Task with Varying Temporal Memory Load. Front. Psychol. *6*, 2031.
31. Bueti, D., and Walsh, V. (2009). The parietal cortex and the representation of time, space, number and other magnitudes. Philos. Trans. R. Soc. Lond. B Biol. Sci. *364*, 1831–1840.
32. Gallistel, C.R. (2011). Chapter 1 - Mental Magnitudes. In Space, Time and Number in the Brain, S. Dehaene and E.M. Brannon, eds. (San Diego: Academic Press), pp. 3–12.
33. Gallistel, C.R., and Gelman, I.I. (2000). Non-verbal numerical cognition: from reals to integers. Trends Cogn. Sci. *4*, 59–65.
34. Walsh, V. (2003). A theory of magnitude: common cortical metrics of time, space and quantity. Trends Cogn. Sci. *7*, 483–488.
35. Klimesch, W., Doppelmayr, M., Schwaiger, J., Auinger, P., and Winkler, T. (1999). 'Paradoxical' alpha synchronization in a memory task. Brain Res. Cogn. Brain Res. *7*, 493–501.
36. Scheeringa, R., Petersson, K.M., Oostenveld, R., Norris, D.G., Hagoort, P., and Bastiaansen, M.C.M. (2009). Trial-by-trial coupling between EEG and BOLD identifies networks related to alpha and theta EEG power increases during working memory maintenance. Neuroimage *44*, 1224–1238.
37. van Ede, F., Chekroud, S.R., Stokes, M.G., and Nobre, A.C. (2018). Decoding the influence of anticipatory states on visual perception in the presence of temporal distractors. Nat. Commun. *9*, 1449.
38. Kornblith, S., Buschman, T.J., and Miller, E.K. (2016). Stimulus Load and Oscillatory Activity in Higher Cortex. Cereb. Cortex *26*, 3772–3784.
39. Tuladhar, A.M., ter Huurne, N., Schoffelen, J.M., Maris, E., Oostenveld, R., and Jensen, O. (2007). Parieto-occipital sources account for the increase in alpha activity with working memory load. Hum. Brain Mapp. *28*, 785–792.
40. Kaufman, L., Curtis, S., Wang, J.-Z., and Williamson, S.J. (1992). Changes in cortical activity when subjects scan memory for tones. Electroencephalogr. Clin. Neurophysiol. *82*, 266–284.
41. Krause, C.M., Lang, A.H., Laine, M., Kuusisto, M., and Pörn, B. (1996). Event-related. EEG desynchronization and synchronization during an auditory memory task. Electroencephalogr. Clin. Neurophysiol. *98*, 319–326.
42. Leiberg, S., Lutzenberger, W., and Kaiser, J. (2006). Effects of memory load on cortical oscillatory activity during auditory pattern working memory. Brain Res. *1120*, 131–140.
43. Obleser, J., Wöstmann, M., Hellbernd, N., Wilsch, A., and Maess, B. (2012). Adverse Listening Conditions and Memory Load Drive a Common Alpha Oscillatory Network. J. Neurosci. *32*, 12376–12383.
44. Wilsch, A., and Obleser, J. (2016). What works in auditory working memory? A neural oscillations perspective. Brain Res. *1640*, 193–207.
45. Chen, X., Ma, R., Zhang, W., Zeng, G.Q., Wu, Q., Yimiti, A., Xia, X., Cui, J., Liu, Q., Meng, X., et al. (2023). Alpha oscillatory activity is causally linked to working memory retention. PLoS Biol. *21*, e3001999.

46. Krause, C.M., Lang, H., Laine, M., Kuusisto, M., and Pörn, B. (1995). Cortical processing of vowels and tones as measured by event-related desynchronization. Brain Topogr. *8*, 47–56.

47. Bonnefond, M., and Jensen, O. (2012). Alpha oscillations serve to protect working memory maintenance against anticipated distracters. Curr. Biol. *22*, 1969–1974.

48. Klimesch, W., Sauseng, P., and Hanslmayr, S. (2007). EEG alpha oscillations: the inhibition-timing hypothesis. Brain Res. Rev. *53*, 63–88.

49. Schneider, D., Herbst, S.K., Klatt, L.-I., and Wöstmann, M. (2022). Target enhancement or distractor suppression? Functionally distinct alpha oscillations form the basis of attention. Eur. J. Neurosci. *55*, 3256–3265. https://doi.org/10.1111/ejn.15309.

50. Chen, F.-W., Li, C.-H., and Kuo, B.-C. (2023). Temporal expectation based on the duration variability modulates alpha oscillations during working memory retention. Neuroimage *265*, 119789.

51. Wilsch, A., Henry, M.J., Herrmann, B., Maess, B., and Obleser, J. (2015). Alpha Oscillatory Dynamics Index Temporal Expectation Benefits in Working Memory. Cereb. Cortex *25*, 1938–1946. https://doi.org/10.1093/cercor/bhu004.

52. Petzschner, F.H., Glasauer, S., and Stephan, K.E. (2015). A Bayesian perspective on magnitude estimation. Trends Cogn. Sci. *19*, 285–293.

53. Lejeune, H., and Wearden, J.H. (2009). Vierordt's The Experimental Study of the Time Sense (1868) and its legacy. Eur. J. Cogn. Psychol. *21*, 941–960.

54. Vierordt, K. (1868). Der Zeitsinn Nach Versuchen (H. Laupp).

55. Grosse-Wentrup, M., and Buss, M. (2008). Multiclass common spatial patterns and information theoretic feature extraction. IEEE Trans. Biomed. Eng. *55*, 1991–2000.

56. Koles, Z.J. (1991). The quantitative extraction and topographic mapping of the abnormal components in the clinical EEG. Electroencephalogr. Clin. Neurophysiol. *79*, 440–447.

57. Shrout, P.E., and Bolger, N. (2002). Mediation in experimental and nonexperimental studies: new procedures and recommendations. Psychol. Methods *7*, 422–445.

58. Van Wassenhove, V. (2009). Minding time in an amodal representational space. Philos. Trans. R. Soc. Lond. B Biol. Sci. *364*, 1815–1830.

59. Bays, P.M., Catalao, R.F.G., and Husain, M. (2009). The precision of visual working memory is set by allocation of a shared resource. J. Vis. *9*, 7.1–7.11.

60. Joseph, S., Teki, S., Kumar, S., Husain, M., and Griffiths, T.D. (2016). Resource allocation models of auditory working memory. Brain Res. *1640*, 183–192.

61. Diaz, G.K., Vogel, E.K., and Awh, E. (2021). Perceptual Grouping Reveals Distinct Roles for Sustained Slow Wave Activity and Alpha Oscillations in Working Memory. J. Cogn. Neurosci. *33*, 1354–1364.

62. Fukuda, K., Mance, I., and Vogel, E.K. (2015). α Power Modulation and Event-Related Slow Wave Provide Dissociable Correlates of Visual Working Memory. J. Neurosci. *35*, 14009–14016.

63. Fukuda, K., and Woodman, G.F. (2017). Visual working memory buffers information retrieved from visual long-term memory. Proc. Natl. Acad. Sci. USA *114*, 5306–5311.

64. Cooper, N.R., Croft, R.J., Dominey, S.J.J., Burgess, A.P., and Gruzelier, J.H. (2003). Paradox lost? Exploring the role of alpha oscillations during externally vs. internally directed attention and the implications for idling and inhibition hypotheses. Int. J. Psychophysiol. *47*, 65–74.

65. Jensen, O., and Mazaheri, A. (2010). Shaping functional architecture by oscillatory alpha activity: gating by inhibition. Front. Hum. Neurosci. *4*, 186.

66. Zhou, Y.J., Ramchandran, A., and Haegens, S. (2023). Alpha oscillations protect working memory against distracters in a modality-specific way. Neuroimage *278*, 120290.

67. Teki, S., and Griffiths, T.D. (2016). Brain Bases of Working Memory for Time Intervals in Rhythmic Sequences. Front. Neurosci. *10*, 239.

68. Harvey, B.M., Dumoulin, S.O., Fracasso, A., and Paul, J.M. (2020). A Network of Topographic Maps in Human Association Cortex Hierarchically Transforms Visual Timing-Selective Responses. Curr. Biol. *30*, 1424–1434.e6.

69. Protopapa, F., Hayashi, M.J., Kulashekhar, S., van der Zwaag, W., Battistella, G., Murray, M.M., Kanai, R., and Bueti, D. (2019). Chronotopic maps in human supplementary motor area. PLoS Biol. *17*, e3000026.

70. Foster, J.J., Sutterer, D.W., Serences, J.T., Vogel, E.K., and Awh, E. (2017). Alpha-Band Oscillations Enable Spatially and Temporally Resolved Tracking of Covert Spatial Attention. Psychol. Sci. *28*, 929–941.

71. Jones, H.M., Diaz, G.K., Ngiam, W.X.Q., and Awh, E. (2024). Electroencephalogram Decoding Reveals Distinct Processes for Directing Spatial Attention and Encoding Into Working Memory. Psychol. Sci. *35*, 1108–1138.

72. Rattat, A.-C., and Droit-Volet, S. (2012). What is the best and easiest method of preventing counting in different temporal tasks? Behav. Res. Methods *44*, 67–80.

73. Helson, H. (1930). The Tau Effect—an Example of Psychological Relativity. Science *71*, 536–537.

74. Bastos, A.M., Loonis, R., Kornblith, S., Lundqvist, M., and Miller, E.K. (2018). Laminar recordings in frontal cortex suggest distinct layers for maintenance and control of working memory. Proc. Natl. Acad. Sci. USA *115*, 1117–1122.

75. Lundqvist, M., Rose, J., Herman, P., Brincat, S.L., Buschman, T.J., and Miller, E.K. (2016). Gamma and Beta Bursts Underlie Working Memory. Neuron *90*, 152–164.

76. Spitzer, B., and Haegens, S. (2017). Beyond the Status Quo: A Role for Beta Oscillations in Endogenous Content (Re)Activation. eNeuro *4*. ENEURO.0170-17.2017.

77. Liljefors, J., Almeida, R., Rane, G., Lundström, J.N., Herman, P., and Lundqvist, M. (2024). Distinct functions for beta and alpha bursts in gating of human working memory. Nat. Commun. *15*, 8950.

78. Salazar, R.F., Dotson, N.M., Bressler, S.L., and Gray, C.M. (2012). Content-Specific Fronto-Parietal Synchronization During Visual Working Memory. Science *338*, 1097–1100. https://doi.org/10.1126/science.1224000.

79. Kononowicz, T.W. (2015). Dopamine-dependent oscillations in frontal cortex index "start-gun" signal in interval timing. Front. Hum. Neurosci. *9*, 331.

80. Kononowicz, T.W., Roger, C., and van Wassenhove, V. (2019). Temporal Metacognition as the Decoding of Self-Generated Brain Dynamics. Cereb. Cortex *29*, 4366–4380. https://doi.org/10.1093/cercor/bhy318.

81. Kulashekhar, S., Pekkola, J., Palva, J.M., and Palva, S. (2016). The role of cortical beta oscillations in time estimation. Hum. Brain Mapp. *37*, 3262–3281.

82. Grabot, L., Kononowicz, T.W., la Tour, T.D., Gramfort, A., Doyère, V., and van Wassenhove, V. (2019). The strength of alpha-beta oscillatory coupling predicts motor timing precision. J. Neurosc., 2473–2518. https://doi.org/10.1523/JNEUROSCI.2473-18.2018.

83. Spitzer, B., Gloel, M., Schmidt, T.T., and Blankenburg, F. (2014). Working memory coding of analog stimulus properties in the human prefrontal cortex. Cereb. Cortex *24*, 2229–2236.

84. Fujioka, T., Trainor, L.J., Large, E.W., and Ross, B. (2012). Internalized Timing of Isochronous Sounds Is Represented in Neuromagnetic Beta Oscillations. J. Neurosci. *32*, 1791–1802.

85. Jha, A., Nachev, P., Barnes, G., Husain, M., Brown, P., and Litvak, V. (2015). The Frontal Control of Stopping. Cereb. Cortex *25*, 4392–4406.

86. Khanna, P., and Carmena, J.M. (2017). Beta band oscillations in motor cortex reflect neural population signals that delay movement onset. eLife *6*, e24573.

87. Zhang, Y., Chen, Y., Bressler, S.L., and Ding, M. (2008). Response preparation and inhibition: The role of the cortical sensorimotor beta rhythm. Neuroscience *156*, 238–246.

88. Brinkman, L., Stolk, A., Dijkerman, H.C., de Lange, F.P., and Toni, I. (2014). Distinct Roles for Alpha- and Beta-Band Oscillations during Mental Simulation of Goal-Directed Actions. J. Neurosci. *34*, 14783–14792.

89. Goldman-Rakic, P.S. (1995). Cellular basis of working memory. Neuron *14*, 477–485.

90. Sprague, T.C., Ester, E.F., and Serences, J.T. (2014). Reconstructions of Information in Visual Spatial Working Memory Degrade with Memory Load. Curr. Biol. *24*, 2174–2180.

91. Lundqvist, M., Miller, E.K., Nordmark, J., Liljefors, J., and Herman, P. (2024). Beta: bursts of cognition. Trends Cogn. Sci. *28*, 662–676.

92. Brainard, D.H. (1997). The Psychophysics Toolbox. Spat. Vis. *10*, 433–436.

93. Pelli, D.G. (1997). The VideoToolbox software for visual psychophysics: Transforming numbers into movies. Spat. Vis. *10*, 437–442.

94. Gramfort, A., Luessi, M., Larson, E., Engemann, D.A., Strohmeier, D., Brodbeck, C., Goj, R., Jas, M., Brooks, T., Parkkonen, L., and Hämäläinen, M. (2013). MEG and EEG data analysis with MNE-Python. Front. Neurosci. *7*, 267.

95. Gramfort, A., Luessi, M., Larson, E., Engemann, D.A., Strohmeier, D., Brodbeck, C., Parkkonen, L., and Hämäläinen, M.S. (2014). MNE software for processing MEG and EEG data. Neuroimage *86*, 446–460.

96. Larson, E., Gramfort, A., Engemann, D.A., Leppakangas, J., Brodbeck, C., Jas, M., Brooks, T.L., Sassenhagen, J., McCloy, D., Luessi, M., et al. (2024). MNE-Python. Zenodo. https://doi.org/10.5281/zenodo.13340330.

97. Appelhoff, S., Sanderson, M., Brooks, T.L., van Vliet, M., Quentin, R., Holdgraf, C., Chaumon, M., Mikulan, E., Tavabi, K., Höchenberger, R., et al. (2019). MNE-BIDS: Organizing electrophysiological data into the BIDS format and facilitating their analysis. J. Open Source Softw. *4*, 1896.

98. R Core Team (2024). R: A Language and Environment for Statistical Computing (Vienna, Austria: R Foundation for Statistical Computing). https://www.R-project.org/.

99. Posit Team (2025). RStudio: Integrated Development Environment. Environ. R Posit Softw. PBC Boston MA. http://www.posit.co/.

100. Dale, A.M., Fischl, B., and Sereno, M.I. (1999). Cortical surface-based analysis I. Segmentation and surface reconstruction. Neuroimage *9*, 179–194.

101. Westner, B.U., and King, J.-R. (2023). The best of two worlds: Decoding and source-reconstructing M/EEG oscillatory activity with a unique model. Preprint at bioRxiv. https://doi.org/10.1101/2023.03.24.534080.

102. Henrich, J., Heine, S.J., and Norenzayan, A. (2010). The weirdest people in the world? Behav. Brain Sci. *33*, 61–83. discussion 83-135.

103. Niso, G., Gorgolewski, K.J., Bock, E., Brooks, T.L., Flandin, G., Gramfort, A., Henson, R.N., Jas, M., Litvak, V., Moreau, J.T., et al. (2018). MEG-BIDS, the brain imaging data structure extended to magnetoencephalography. Sci. Data *5*, 180110.

104. Bates, D., Mächler, M., Bolker, B., and Walker, S. (2015). Fitting Linear Mixed-Effects Models Using lme4. J. Stat. Softw. *67*, 1–48.

105. Kuznetsova, A., Brockhoff, P.B., and Christensen, R.H.B. (2016). lmerTest: tests in linear mixed effects models. https://www.jstatsoft.org/article/view/v082i13.

106. Makowski, D., Ben-Shachar, M.S., and Lüdecke, D. (2019). bayestestR: Describing Effects and their Uncertainty, Existence and Significance within the Bayesian Framework. J. Open Source Softw. *4*, 1541.

107. Wagenmakers, E.-J. (2007). A practical solution to the pervasive problems ofp values. Psychon. Bull. Rev. *14*, 779–804.

108. Lee, M.D., and Wagenmakers, E.-J. (2014). Bayesian Cognitive Modeling: A Practical Course (Cambridge University Press).

109. Rouder, J.N., Speckman, P.L., Sun, D., Morey, R.D., and Iverson, G. (2009). Bayesian t tests for accepting and rejecting the null hypothesis. Psychon. Bull. Rev. *16*, 225–237.

110. Taulu, S., and Kajola, M. (2005). Presentation of electromagnetic multichannel data: The signal space separation method. J. Appl. Phys. *97*, 124905.

111. Dammers, J., Schiek, M., Boers, F., Silex, C., Zvyagintsev, M., Pietrzyk, U., and Mathiak, K. (2008). Integration of amplitude and phase statistics for complete artifact removal in independent components of neuromagnetic recordings. IEEE Trans. Biomed. Eng. *55*, 2353–2362.

112. Tallon-Baudry, C., Bertrand, O., Delpuech, C., and Pernier, J. (1996). Stimulus specificity of phase-locked and non-phase-locked 40 Hz visual responses in human. J. Neurosci. *16*, 4240–4249.

113. Haufe, S., Meinecke, F., Görgen, K., Dähne, S., Haynes, J.D., Blankertz, B., and Bießmann, F. (2014). On the interpretation of weight vectors of linear models in multivariate neuroimaging. Neuroimage *87*, 96–110.

114. Van Veen, B.D., Van Drongelen, W., Yuchtman, M., and Suzuki, A. (1997). Localization of brain electrical activity via linearly constrained minimum variance spatial filtering. IEEE Trans. Biomed. Eng. *44*, 867–880.

115. Dale, A.M., Liu, A.K., Fischl, B.R., Buckner, R.L., Belliveau, J.W., Lewine, J.D., and Halgren, E. (2000). Dynamic statistical parametric mapping: combining fMRI and MEG for high-resolution imaging of cortical activity. Neuron *26*, 55–67.

116. Destrieux, C., Fischl, B., Dale, A., and Halgren, E. (2010). Automatic parcellation of human cortical gyri and sulci using standard anatomical nomenclature. Neuroimage *53*, 1–15.

117. Tibshirani, R.J., and Efron, B. (1993). An introduction to the bootstrap. Monogr. Stat. Appl. Probab. *57*, 1–436.

118. Grandchamp, R., and Delorme, A. (2011). Single-Trial Normalization for Event-Related Spectral Decomposition Reduces Sensitivity to Noisy Trials. Front. Psychol. *2*, 236.

119. Baron, R.M., and Kenny, D.A. (1986). The Moderator-Mediator Variable Distinction in Social Psychological Research. Conceptual, Strategic, and Statistical Considerations. J. Pers. Soc. Psychol. *51*, 1173–1182.

120. Benwell, C.S.Y., Keitel, C., Harvey, M., Gross, J., and Thut, G. (2018). Trial-by-trial co-variation of pre-stimulus EEG alpha power and visuospatial bias reflects a mixture of stochastic and deterministic effects. Eur. J. Neurosci. *48*, 2566–2584.

121. Memon, M.A., Jun, H.C., Ting, H., and Francis, C.W. (2018). Mediation analysis issues and recommendations. J. Appl. Struct. Equation Model. *2*. i–ix.

122. Muller, D., Judd, C.M., and Yzerbyt, V.Y. (2005). When moderation is mediated and mediation is moderated. J. Pers. Soc. Psychol. *89*, 852–863.

123. Seabold, S., and Perktold, J. (2010). Statsmodels: Econometric and Statistical Modeling with Python. scipy. https://doi.org/10.25080/Majora-92bf1922-011.

STAR★METHODS

KEY RESOURCES TABLE

REAGENT or RESOURCE	SOURCE	IDENTIFIER
Deposited data		
Behavioral Data (.Rda) and Custom Code	Open Science Framework	Project: p6m7s https://doi.org/10.17605/OSF.IO/P6M7S
MEG Data (BIDS format)	OpenNeuro	Dataset: DS006720 https://doi.org/10.18112/openneuro.ds006720.v1.0.0
Software and algorithms		
MATLAB 2017a	The Mathworks	https://mathworks.com
Psychtoolbox	Brainard[92]; Pelli[93]	http://psychtoolbox.org/
MNE Python version 1.8.0,	Gramfort et al.,[94,95] Larson et al.[96]	https://mne.tools/stable/index.html
MNE-BIDS version 1.6.0	Appelhoff et al.[97]	https://mne.tools/mne-bids/stable/index.html
MNE-BIDS-Pipeline v. 1.8	N/A	https://mne.tools/mne-bids-pipeline/
R version 4.3.3 and version 4.5.0	R Core Team[98]	https://www.r-project.org/
RStudio version 2025.5.0.496	Posit Team 2025[99]	https://posit.co/download/rstudio-desktop/
Freesurfer	Dale et al.[100]	https://surfer.nmr.mgh.harvard.edu/fswiki/FreeSurferWiki
Source projection code for CSD patterns	Westner & King[101]	https://github.com/britta-wstnr/source_decoding
Custom Code	Deposited on OFS	https://doi.org/10.17605/OSF.IO/P6M7S

EXPERIMENTAL MODEL AND STUDY PARTICIPANT DETAILS

Twenty-three participants (14 women, mean age = 26.2 years, SD = 5.2 years) were recruited at Neurospin. The sample size was chosen in accordance to previous behavioral experiments.[15] All participants were right-handed, and had normal hearing and vision, and no self-reported history of audiological or neurological disorders. Participants were naive as to the purpose of the study and received monetary compensation for their participation. Prior to the study, all participants signed a written informed consent in accordance with the Ethics Committee on Human Research at Neurospin: CPP n° 100049 (Gif-sur-Yvette, France), and the Declaration of Helsinki (2013). Three participants were excluded, one because of a problem with the triggers, one had incomplete data, and for the third, no anatomical MRI scan was available. This left 20 participants for the analyses.

This study addresses general cognitive mechanisms that are not expected to be influenced by sex or gender, and it is not common practice to assess such influences in this area of human cognitive neuroscience without an *a priori* hypothesis. Furthermore, the small sample size, and the non-availability of additional information (such as hormonal cycle phase in female participants), would have made analyses by sex or gender unreliable. Ancestry, race, ethnicity, and socioeconomic status of participants were not recorded, as this information is considered sensitive data under French law and was not covered by the current ethics approval. While the sample characteristics are standard for resource-intensive neuroimaging studies aiming for relatively small, homogeneous samples, they have been criticized for not reflecting the worldwide population.[102] Given the targeted age group, participants were likely either university students or young professionals, which may have biased the sample's socioeconomic status. While there is *a priori* no reason to assume that basic neural and behavioural markers like the ones assessed here should be affected by these individual characteristics, future research should extend these findings to more diverse populations, particularly a wider age group.

METHOD DETAILS

General procedure and task

Participants performed an *n-item delayed temporal reproduction* task.[15] They were presented with a sequence of one or three "empty" intervals (Figure 1A), delimited by short pure tones (*encoding*; for details about the stimuli see below). Empty time intervals were used to prevent a maintenance strategy based on auditory features, as opposed to duration. They had to maintain the sequence in memory (*retention*), and, upon a prompt, reproduce the whole sequence by pressing a button for each tone (*reproduction*). Participants received feedback after each reproduction of a sequence.

Before the main experiment, the researcher explained the task to the participants, and provided them with written instructions. Participants then started a training block composed of eight trials. The training was repeated if a participant failed on more than half of the trials (average relative temporal reproduction error over all items in the sequence below - 0.5 or above + 0.5). Data

from the training session were not included in the analyses. The actual experiment consisted of 8 blocks of 36 trials each; each block lasted about 10 minutes. After each block, the MEG recording was stopped to save the data, resulting in a break for the participant. The total MEG session lasted 90 minutes. Each participant was presented with the same conditions, in randomized order as described above. As the design was a repeated-measures within subject design, no blinding was put in place.

Stimuli

The experimental paradigm was adapted from Experiment 2 in Herbst et al.[15] All stimuli were created digitally using Psychtoolbox (Brainard, 1997) under MATLAB (2017a, The Mathworks), at a sampling rate of 44.1 kHz. Stimuli consisted of a sequence of pure tones (1 kHz, 50 ms duration including 10 ms onset and offset ramping to avoid onset artifacts), which demarcated the time intervals (hereafter referred to as "items").

Three sequence durations were tested (1.6 s, 2.4 s and 3.6 s) and the number of duration items was one or three for each sequence. Two-item sequences as used in the previous behavioral study were removed to obtain more trials per condition in the MEG experiment. The order of items within each n-item sequence was randomized. We orthogonalized n-items and the duration of the sequences, resulting in a fixed sequence duration regardless of n-items, but shorter individual items in sequences with more items (Figure 1B). Each block contained all possible sequence types in random order: for the 3-item sequences, six permutations of the order exist for each of the three sequence durations (18 trials), and the three different 1-item sequences were each repeated six times throughout the block, to balance the number of 1- and 3-item sequences.

During encoding, a red fixation dot was displayed on the center of the screen. 0.5 s after the last tone in the sequence, an orange fixation dot signaled the onset of the retention period. The retention period lasted for 4.2 s. This relatively long interval was chosen with the aim to assess the neural dynamics of working memory with MEG during a period free from sensory stimuli. Following the retention period, a green fixation dot prompted participants to reproduce the full sequence. To respond, participants pressed one button on a Fiber Optic Response Pad (FORP, Science Plus Group, DE) with the index finger of their right hand. Participants had unlimited time to initiate their reproduction, and no sounds were played when they pressed the button.

To reproduce the sequence, participants pressed the button as many times as there were tones in the sequence (e.g., 4 key presses for 3 items demarcated by 4 tones), trying to reproduce each duration as precisely as possible. If the correct number of presses was registered, visual feedback was displayed on the screen 0.5 s after the last button press. Visual feedback was displayed for 1 s, and followed by a variable inter-trial interval sampled from a uniform distribution ranging from 2 s to 3 s. Feedback was given in the form of a visual bar plot, which depicted the relative signed reproduction error for each item in the sequence: (item reproduction – item duration)/item duration. Thus, bars of zero length indicated perfectly accurate reproduction, while bars above and below zero reflected over- and under-reproduction, respectively. Trials in which the participant pressed too early (during retention), or an incorrect number of times were labelled as error trials and the participant was prompted with 'too early'/'wrong number of clicks' instead of the feedback described above. These trials were removed from the analyses.

MEG recording

Prior to the arrival of the participant, an empty room recording was performed for one minute to assess the noise level of the MEG sensors. Before undergoing the MEG recording, participants were equipped with external electrodes, positioned to record the electro-occulogram (EOG, horizontal and vertical eye movements) and -cardiogram (ECG). The positions of the EEG electrodes, four head-position indicator coils, and three fiducial points (nasion, left and right pre-auricular areas) were digitized using a 3D digitizer (Polhemus, US/Canada) for subsequent co-registration with the individual's anatomical MRI. The MEG recordings took place in a magnetically shielded chamber, where the participant was seated in an armchair under the MEG helmet. The electromagnetic brain activity was recorded using a whole-head Elekta Neuromag Vector View 306 MEG system (Neuromag Elekta LTD, Helsinki) with 102 triple-sensors elements (two orthogonal planar gradiometers, and one magnetometer per sensor location). Participants were instructed to fixate their gaze on a screen positioned in front of them, at about one meter distance. The chamber was dimly lit. Their head position was measured before each recording run (8 in total) using the head-position indicator coils. MEG recordings were sampled online at 1 kHz, high-pass filtered at 0.03 Hz, and low-pass filtered at 330 Hz. A two-minute-long resting state recording (eyes open) was performed after the task, used to compute the noise covariance matrix for source reconstruction.

Anatomical MRI recordings

To improve the spatial resolution of the source reconstruction, individual high-resolution structural Magnetic Resonance Imaging (MRI) recordings were used. These were recorded on another day, using a Siemens 3 T Magnetom Prisma Fit MRI scanner. Parameters of the sequence were: slice thickness: 1 mm, repetition time TR = 2300 ms, echo time TE = 2.98 ms, and flip angle = 9 degrees.

QUANTIFICATION AND STATISTICAL ANALYSIS

Software

The analyses of the behavioral data were conducted using R version 4.3.3.[98] The MEG data were analyzed using MNE Python (version 1.8.0),[94–96] transformed to the standardized brain imaging data structure (BIDS)[103] using MNE BIDS (version 1.6.0),[97] and

analyzed with the MNE BIDS pipeline (version 1.8, https://mne.tools/mne-bids-pipeline/), plus additional custom-written code. FreeSurfer was used for the reconstruction of the MRI surfaces.[100]

Behavioral data

The reproduced duration per item was measured as the time between the onsets of the two key presses. We removed reproduction outliers defined as reproductions that exceeded by 3 standard deviations the participant's mean reproduction for that duration. Recall precision is commonly used in working memory experiments as a continuous measure of working memory load.[20] To ensure that our measure of precision was not confounded by established biases in reproducing durations with varying magnitudes, we employed the **coefficient of variation (CV)**, a widely accepted index of precision in timing research.[11] We computed CV for bins of items of the same duration, and from the same n-item sequence for each participant as follows:

$$\boldsymbol{CV} = \frac{SD(item\ reproduction)}{mean(item\ reproduction)}$$

To be in accordance with previous studies, we also computed the **relative reproduction** per item (**relRP**), in the same bins as CV, defined as follows:

$$\boldsymbol{relRP} = \frac{item\ reproduction}{item\ duration}$$

Parallel statistical analyses were performed on **relRP** and **CV**, testing for effects of the number of items (n-items), sequence duration, and their interaction. Random intercepts and slopes were included for all predictors. To assess statistical significance, we computed linear mixed effect models using R's *lme4* package,[104] with the Satterthwaite approximation of degrees of freedom, implemented in the *lmerTest* package.[105] Additionally, to obtain effect sizes and assess null-effects, we computed Bayes factors (BF) for each predictor in the model using the *bayestestR* package[106] via the Bayesian Information Criterion approximation.[107] The alpha level for assuming statistical significance was set to $p < 0.05$. In addition, we use Bayes factors to support an unequivocal interpretation of the results. BF represent the relative posterior probability of observing the data under the alternative (i.e., full) and null (i.e., reduced) model, which is informative about whether the inclusion of a given predictor into the model improves the explained variance. For BF we chose the criterion of >3 and <0.3 when comparing to models.[108,109] BF between 0.3 and 3 reflect inconclusive outcomes. In Table 1, we report F- and p-values, as well as BF. In the figures, significance values are marked with asterisks, indicating * $p < 0.05$ and ** $p < 0.01$.

MEG preprocessing

To remove artifacts from the recorded data, we used a standardized preprocessing routine, implemented in the MNE-BIDS-pipeline, with the following steps: noisy or flat sensors were identified visually and marked for exclusion. Next, environmental artifacts were removed from the raw data, using signal source separation (SSS or Maxwell-filter),[110] which also interpolates the bad sensors. Head position coordinates were read from the first of the eight recording runs, and all other runs were spatially aligned to these coordinates. The data were then filtered with a low-pass filter of 160 Hz, and a notch-filter at 50, 100, and 150 Hz to remove line noise. No additional high-pass filter was applied (0.03 Hz used during recording). Furthermore, we resampled the data to a sampling frequency of 250 Hz to speed up the subsequent computations.

Next, the data were cut into epochs of -5 s to 10 s around the onset of the retention interval, and epochs with peak-to-peak amplitudes exceeding 50,000 fT in the magnetometers were rejected. We deliberately used no baseline for the time-domain data, as the interval preceding the retention interval contains the evoked activity from the last tone presented during the encoding phase, and the encoding phase itself varies in duration because of the different sequence durations. Independent component analysis (ICA) was performed on the remaining epochs, with an additional 1 Hz high-pass filter applied only for that purpose. For the detection of artefacts related to the electro-occulogram (EOG) and -cardiogram (ECG), we used an inbuilt routine in MNE python, which finds a participant's typical EOG and ECG activity recorded with the external electrodes, and returns the ICA components that correlate with these typical events. Thresholds for returning the ICA components were set to: 0.1 for the ECG (cross-trial phase statistics),[111] and 4.0 for the EOG (z-score).

After ICA cleaning, we rejected epochs with peak-to-peak amplitudes exceeding 10,000 fT (magnetometers) and 20,000 fT/cm (gradiometers). In the following, we report only the analyses of the 102 magnetometers, to reduce the dimensionality of the data and simplify the interpretation of the results and topographies. On average, we obtained 271.7 clean epochs per participant (SD = 13.45, minimum: 246, maximum: 288).

Anatomical MRI preprocessing and forward model computation

FreeSurfer's "recon-all" function was used to reconstruct the cortical surfaces of each participant's brain. Individual surfaces were mapped to FreesSurfer's 'fsaverage' template brain, for later averaging. Single-layer individual head models were computed using the boundary element method (watershed BEM), from each participant's aMRI. The coregistration of the MEG data with the individual's structural MRI was carried out by manually realigning the digitized fiducial points with the anatomical landmarks of the head surface reconstructed from the MRI (using MNE Python's command coregistration gui). Second, an iterative refinement procedure

was used to realign all digitized points with the individuals' scalp. We then computed a surface-based source space with 4098 candidate dipoles per hemisphere, spaced approximately 4.9 mm apart (24 mm^2 per source area; recursively subdivided octahedrons 'oct6'), a minimal distance of 5 mm from the inner skull. The final forward models were derived from this source space, the co-registration matrices, and the boundary element models.

Common spatial pattern decoding

To investigate how duration sequences are represented in working memory and identify the factors contributing to memory load, we focused our MEG data analysis on the retention interval. During this period devoid of sensory inputs, we examined how sequences varying in length and duration modulate *induced oscillatory activity*,[112] in line with established neural dynamics of working memory.[21] We employed a decoding approach using Common Spatial Patterns (CSP) in combination with logistic regression, implemented as part of the MNE BIDS pipeline. CSP is recommended for the analysis of induced oscillatory activity.[55,56] It identifies spatial filters that maximize the variance of one class of signals (e.g., sequences with a three versus one item), while minimizing the variance of other classes. This allowed us to effectively classify brain activity patterns associated with varying memory load.

We performed the CSP spatial filtering in linearly spaced time-frequency bins, ranging from 2 – 30 Hz (bin width of 2 Hz, 14 bins) and 0.5 – 4 s following retention onset (bin width of 0.25 s, 14 bins). Specifically, the filtering and decoding was run on each trials' covariance matrix computed on single trial data, band-pass filtered in the range of the desired frequency bin, after subtracting the evoked response to focus on induced activity. Since no time-frequency transformation is performed here, there was also no additional baseline-correction. For decoding, we used logistic regression (solver: "liblinear") with a 5-fold cross validation (shuffled splits), and quantified decoding performance as the area under the receiver-operator curve averaged across the folds.

To assess in which frequency bands and at which time points we could significantly decode the number of items or the sequence duration at the group level, we performed cluster-permutation tests on the decoding accuracy values across time-frequency bins, using an initial cluster forming threshold of $p < 0.01$, a final cluster selection threshold of $p < 0.05$, and 5000 permutations.

Source reconstruction

To further investigate which brain areas contribute to the significant decoding accuracy, we reconstructed the sources of the decoding patterns (https://github.com/britta-wstnr/source_decoding).[101] Here, we used the decoding weights (recomputed now for all epochs jointly without cross-validation), and transformed them to the corresponding patterns across sensors (group average depicted in Figure 2C). Topographical patterns are closer to an interpretation as neurophysiological activity compared to the classifier weights.[113] We then computed linearly constrained minimum variance spatial filters (lcmv-beamformers)[114] from the epoched and band-pass filtered data, and a noise covariance matrix from the resting state recording, and projected the decoding patterns (back-transformed to covariance matrices) to the source level. Finally, we morphed the individual source activity to a template brain for averaging (fsaverage). We performed the source reconstruction for the complete range of frequencies identified as statistically significant, and second, split into the canonical alpha (8 – 12 Hz) and beta (15 – 25 Hz) frequency bands. Finally, to investigate the directions of the effects, we also projected the frequency-band power difference (covariance matrix computed from band-pass filtered epochs) for 1-item and 3-item sequences to source space using minimum-norm estimates (dSPM).[115]

Brain-behavior relationships

To further assess whether the neural dynamics identified as correlates of working memory load for durations directly relate to behavioral reproduction precision, we extracted single trial power in the alpha (8 – 12 Hz) and beta (15 – 25 Hz) bands from the occipital, parietal, and central regions, in which we found significant decoding (labels: lateraloccipital, inferiorparietal, superiorparietal, supramarginal, precentral, postcentral from the 'aparc' atlas[116]). We created functional labels for each participant per hemisphere, by subselecting the 15 % of voxels with the highest activity in each label (across all conditions). Selecting only the most activated voxels balanced the need for robust labels, despite individual differences, with the goal of maximizing the signal-to-noise ratio by excluding inactive voxels. We then computed the average power for the alpha and beta band for each label, by applying the Hilbert transform to bandpass-filtered data from each epoch to obtain complex time series, and squaring the absolute values averaging across voxels and time points (0.5 – 4 s) to obtain oscillatory power.

To obtain precision *for each trial*, a measure which is per se defined *across* trials, we applied a resampling and bootstrapping technique.[117] Per participant and n-items, we randomly selected 20 trials (without replacement), and computed one value of CV and average power for this sample. We repeated this 1000 times. To test for significant correlations between power and CV, we computed correlations between CV and power across these 1000 values, and compared them to a null-distribution, for which we shuffled the indices of the 1000 samples and computed the correlation, repeating this shuffling 1000 times to obtain a null-distribution of 1000 correlation values (Table S1; Figure S3). CV was z-scored across all participants and trials for model stability, and power values were averaged for the left and right hemispheres and z-scored per individual, as recommended by e.g., Grandchamp & Delorme.[118] In order to compute p-values, we counted how many correlation values obtained from the null distribution were as large or larger than the true correlation value. We set a threshold of $p < 0.004$ ($p < 0.05$ with Bonferroni correction for 12 comparisons). We targeted only CV for this analysis (and not relRP), as it provides a bias-free measure of recall precision in particular with respect to wide range of durations used.

Mediation analyses

We also assessed whether oscillatory power in the retention window mediates the effect of n-items on CV,[57,119–122] i.e., whether the neural dynamics play the hypothesized statistical role to index working memory load caused by the number of items. To test for the presence of a statistically significant mediation, we followed the steps described in Shrout & Bolger.[57] We used the same resampling technique as above to compute power and CV for 1000 samples for each participant (500 per n-item). We computed linear mixed effect models using the *mixedlm* function from the *statsmodels* package for python.[123] The models were twofold: (1) regressing power on n-items (*a* effect) and (2) regressing CV on power (*b* effect) and n-items (*c'* effect). Both models had a random intercept and random slopes across participant for each fixed effect. From these models, we estimated regression coefficients for the three effects, and repeated the sampling 5000 times to obtain reliable 95% bootstrap confidence intervals.[117] The mediation was quantified as the product of the $a \times b$ effect. If the confidence interval for this effect does not include zero, a significant mediation can be assumed.[57] Results are depicted in Table S2 and Figure S4.